

Exotic Lifshitz transitions in topological materials

G.E. Volovik^{1,2,3}

¹*Low Temperature Laboratory, Aalto University, P.O. Box 15100, FI-00076 AALTO, Finland*

²*L. D. Landau Institute for Theoretical Physics, 117940 Moscow, Russia*

³*P.N. Lebedev Physical Institute, RAS, Moscow 119991, Russia*

(Dated: September 4, 2017)

Topological Lifshitz transitions involve many types of topological structures in momentum and frequency-momentum spaces: Fermi surfaces, Dirac lines, Dirac and Weyl points, etc. Each of these structures has their own topological invariant ($N_1, N_2, N_3, \tilde{N}_3$, etc.), which supports the stability of a given topological structure. The topology of the shape of Fermi surfaces and Dirac lines, as well as the interconnection of the objects of different dimensions, lead to numerous classes of Lifshitz transitions. The consequences of Lifshitz transitions are important in different areas of physics. The singularities emerging at the transition may enhance the transition temperature to superconductivity; the Lifshitz transition can be in the origin of the small masses of elementary particles in our Universe; the black hole horizon serves as the surface of Lifshitz transition between the vacua with type-I and type-II Weyl points; etc.

PACS numbers:

I. INTRODUCTION. FERMI SURFACE, DIRAC LINE, WEYL POINT

The key word in consideration of Lifshitz transitions is topology. Following original Lifshitz paper,¹ Lifshitz transition has been viewed as a change of the topology of the Fermi surface without symmetry breaking. Later it became clear that topology of the shape is not the only topological characterization of the Fermi surface. Fermi surface itself represents the singularity in the Green's function, which is topologically protected: it is the vortex line in the four-dimensional frequency-momentum space in Fig. 1 (*top right*). The stability of the Fermi surface under interaction between the fermions is in the origin of the Fermi liquid theory developed by Landau. Moreover, the Fermi surface appeared to be one in the series of the topologically stable singularities,^{2,3} which include in particular the Weyl point – the hedgehog in momentum space in Fig. 1 (*middle*) and the Dirac line – the vortex line in the three-dimensional momentum space in Fig. 1 (*bottom*). The stability of these objects is supported by the corresponding topological invariants in momentum space or in extended frequency-momentum space.

The combination of topology of the shape of the Fermi surfaces, Fermi lines and Fermi points together with the topology, which supports the stability of these objects, and also the topology of the interconnections of the objects of different dimensions provide a large number of different types of Lifshitz transitions. Examples of Lifshitz transitions coming from the interplay of different topological objects in momentum space are discussed in Refs.⁴⁻⁶ and in Secs. III C and IV. This makes the Lifshitz transitions ubiquitous with applications to high energy physics, cosmology, black hole physics and to search for the room- T superconductivity.

In particular, the Lifshitz transition may give the solution of the hierarchy problem in particle physics: why the masses of elementary particles in our Universe are so

extremely small compared with the characteristic Planck energy scale. Indeed, when we compare the mass $\sim 10^2$ GeV of the most heavy particle – the top quark – with the Planck energy $\sim 10^{19}$ GeV, we can see that the vacuum of our Universe is practically gapless. There are several topological scenarios, which may lead to the (almost) gapless vacuum.

In one scenario the quantum vacuum belongs to the class of the gapless (massless) Weyl materials in Fig. 1 (*middle*), where the nodes in the spectrum of elementary particles – the Weyl points – are topologically protected,^{2,3,9} see Sec. III A and Fig. 9. According to this scenario the physical laws are not fundamental, but emerge in the low energy corner of the quantum vacuum, i.e. in the vicinity of the Weyl points, where the spectrum becomes linear and all the symmetries of Standard Model including Lorentz invariance and general covariance emerge from nothing. In this scenario the Lifshitz transition between type-I and type-II Weyl vacua take place at the black hole horizon, see Sec. III D.

At even lower energy some of these symmetries experience spontaneous breaking, analogous to the superconducting transition. In the latter case the hierarchy problem is understood: in most superconductors the transition temperature T_c is exponentially small, compared to the characteristic Fermi energy scale (analog of the Planck scale), which forces us to search for the exceptional materials with enhanced T_c . The role of the Lifshitz transition in the enhancement of the temperature of superconducting transition is in Sec. II D and Sec. III C.

In the other scenario, the massless (gapless) vacua emerge at the Lifshitz transition between the fully gapped vacua with different topological charges, see Sec. VI and Fig. 18. The almost perfect masslessness of elementary particles in our Universe suggests that the Universe is very close to the line of the topological Lifshitz transition between the fully gapped vacua, at which fermions necessarily become gapless,¹⁰ see Sec. VI. This is the topo-

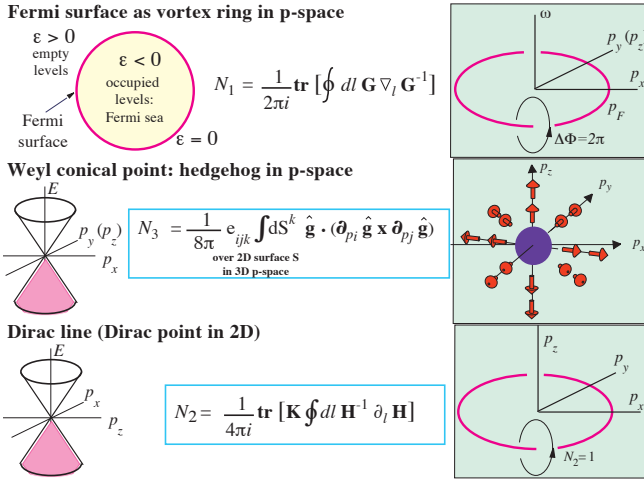


FIG. 1: Topologically stable nodes in the energy spectrum of electrons in metals or fermions in general.

(*Top*): Fermi surface represents the singularity in the Green's function, which forms the vortex in the 3 + 1 (\mathbf{p}, ω) -space, see Sec. II A and Fig. 2 (in the 2 + 1 (p_x, p_y, ω) -space this is the vortex line). The stability of the vortex is supported by the winding number – the integer-valued invariant N_1 , expressed in terms of the Green's function. Lifshitz transitions, which involve the Fermi surface, are discussed in Secs. II and IV.

(*Middle*): Conical point in the fermionic spectrum of the Weyl materials (Weyl semimetals, chiral superfluid $^3\text{He-A}$, and the vacuum of Standard Model in its gapless phase, see Sec. III and Fig. 9). The directions of spin (or of the emergent spin, isospin, pseudo-spin, etc.) form the topological object in momentum space – the hedgehog or the Berry phase monopole⁷ – described by the integer-valued topological invariant N_3 . Lifshitz transitions, which involve the Weyl nodes, are discussed in Secs. III, IV and VI.

(*Bottom*): Dirac lines – lines of zeroes in the energy spectrum, described by the topological invariant N_2 . The circular line is the Dirac line in the quasiparticle spectrum in the polar phase of superfluid ^3He , which has been recently created in aerogel.⁸ The same invariant N_2 stabilizes the point nodes in 2D materials, such as graphene, see Sec.V.

logical analog of the so-called Multiple Point Principle, according to which the Universe lives at the coexistence point (line, surface, etc.) of the first order phase transition, where different vacua have the same energy.^{11–15}

II. FERMI SURFACE AND LIFSHITZ TRANSITIONS

A. Fermi surface as topological object

The primary topology, which is at the origin of the Lifshitz transitions, is the topology which is responsible for the stability of the Fermi surface. If the Fermi surface is not stable under the electron-electron interaction, the consideration of the topology of the shape of the Fermi surface and of the corresponding Lifshitz transitions does

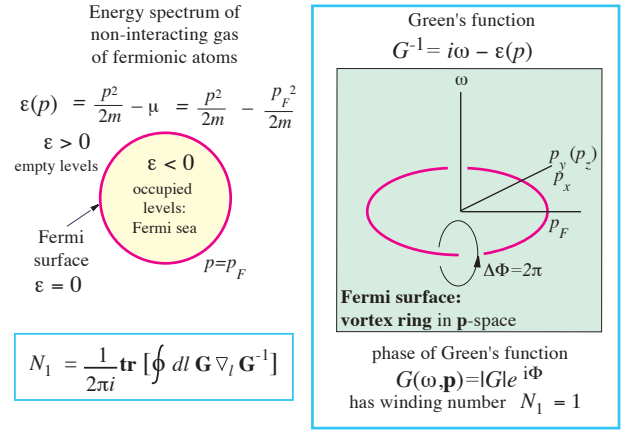


FIG. 2: Fermi surface is robust to interactions because it represents the topologically stable singularity in the Green's function – the vortex in the 3 + 1 (\mathbf{p}, ω) -space. The stability of the vortex is supported by the winding number of the phase Φ of the Green's function $G = |G|e^{i\Phi}$. In general the winding number is given by the integer-valued invariant N_1 , expressed in terms of the Green's function.

not make much sense. To view the topological stability of the Fermi surface with respect to interactions let us start with the Green's function of an ideal Fermi gas in Fig. 2 (*left*). The Fermi surface $\epsilon(\mathbf{p}) = 0$ of the noninteracting Fermi gas is the boundary in momentum space, which separates the occupied states with $\epsilon(\mathbf{p}) < 0$ from the empty states with $\epsilon(\mathbf{p}) > 0$. The Green's function $G(\omega, \mathbf{p})$ with ω on imaginary axis

$$G^{-1}(\omega, \mathbf{p}) = i\omega - \epsilon(\mathbf{p}), \quad (1)$$

has singularity at $\omega = 0$ and $\epsilon(\mathbf{p}) = 0$. In Fig. 2 (*right*) the p_z coordinate is suppressed, and the Green's function singularity forms the closed line in the 2 + 1 momentum-frequency space (p_x, p_y, ω) . This line represents the vortex line, at which the phase of the Green's function $\Phi(p_x, p_y, \omega)$ has the 2π winding. As in the case of the real-space vortex in superfluids, the integer winding number provides the stability of the Fermi surface with respect to perturbations, including the interaction (if the p_z component is restored, the singularity forms the vortex sheet in the 3 + 1 momentum-frequency (\mathbf{p}, ω) space).

In general case, when the Green's function has the spin, band and other indices, the winding number can be written as the following topological invariant in terms of the Green's function:

$$N_1 = \mathbf{tr} \oint_C \frac{dl}{2\pi i} G(\omega, \mathbf{p}) \partial_l G^{-1}(\omega, \mathbf{p}). \quad (2)$$

Here the integral is taken over an arbitrary contour C around the momentum-frequency vortex sheet, and \mathbf{tr} is the trace over all the indices.

Due to topological stability one cannot make a hole in the Fermi surface. As in the case of vortex lines, which cannot terminate in bulk, the Fermi surface has no edges.

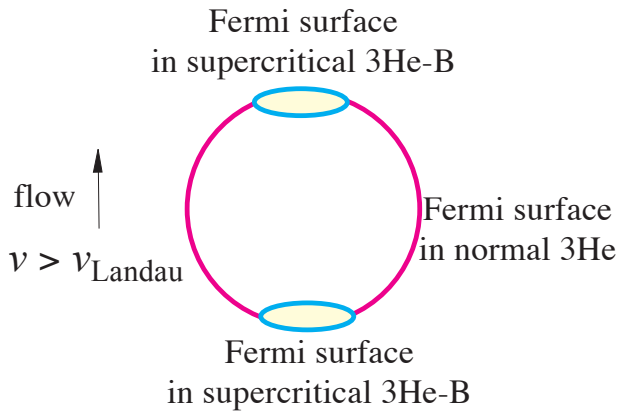


FIG. 3: Lifshitz transition at which the closed Fermi surfaces appear in the fully gapped superfluid $^3\text{He-B}$, when the flow velocity of the liquid with respect to the walls of container exceeds Landau critical velocity.^{3,23}

B. Fermi surface Lifshitz transitions

Because of the topological stability the Fermi surface may be formed even in the superconducting state. The conditions for that are multi-band structure and broken time reversal symmetry T and parity P .^{16–20} These the so-called Bogolubov Fermi surfaces appear also in gapless superfluids, when the Weyl points in $^3\text{He-A}$ and Dirac nodal line in the polar phase of ^3He are inflated to the Fermi pockets in the presence of superflow, which violates both T and P symmetries.^{21,22}

The Fermi surface can be also formed in the fully gapped superfluids, if the velocity of superflow exceeds Landau critical velocity.^{3,23} The crossing of Landau velocity with formation of closed Bogoliubov Fermi surfaces is an example of one of the two transitions suggested by Lifshitz, see Fig. 3.

Another original Lifshitz transition takes place when the Fermi surface crosses the stationary point of the electronic spectrum. Near the transition the expansion of the generic spectrum has the form:¹

$$\epsilon_{\mathbf{p}} = ap_x^2 + bp_y^2 + cp_z^2 - \mu. \quad (3)$$

For $a > 0$, $b > 0$, $c < 0$ the transition with disruption of the neck of the Fermi surface at $\mu = 0$ is in Fig. 4 (*top*). In terms of the vortex singularities of the Green's function in 3+1 (\mathbf{p}, ω) space, this Lifshitz transition represents the interconnection of the vortex lines in Fig. 4 (*bottom*). In superfluids, the interconnection of the real-space vortices is an important process in the vortex turbulence.²⁴

C. From pole of Green's function to zero

While in conventional Landau Fermi liquid the Green's function has a pole, for Luttinger liquid the residue of

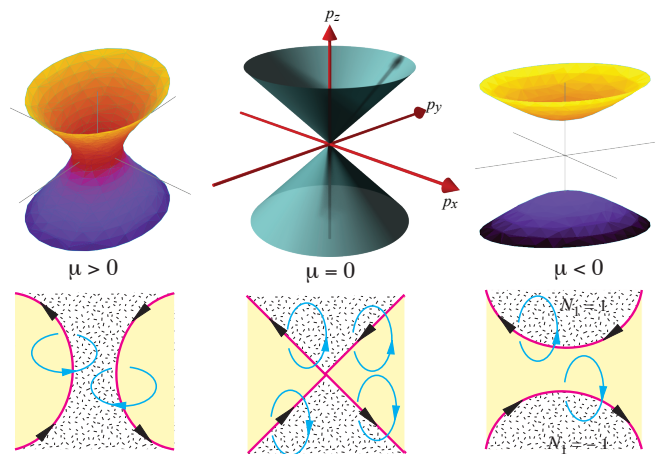


FIG. 4: Since the Fermi surface represents the vortex in the 3+1 (\mathbf{p}, ω) space, the Lifshitz transition with disruption of the neck of the Fermi surface¹ (*top*) is equivalent to the interconnection of vortices in quantum turbulence²⁴ (*bottom*).

From pole of Green's function to zero

non-interacting fermions

$$G = \frac{1}{i\omega - \epsilon(\mathbf{p})}$$

pole



$$N_1 = \frac{1}{4\pi i} \text{tr} \left[\oint dt \mathbf{G} \nabla_l \mathbf{G}^{-1} \right] = 1$$

strongly interacting fermions

$$G = Z \frac{1}{i\omega + \epsilon(\mathbf{p})}$$

zero

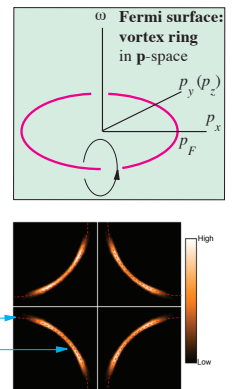


FIG. 5: Lifshitz transition at which the whole Fermi surface of the poles in the Green's function or part of the Fermi surface transforms to the surface of zeroes in the Green's function. The topological charge of the surface does not change at this quantum phase transition. As a result the Luttinger theorem remains valid,^{26,27} i.e. the particle density of interacting fermions is equal to the volume in the momentum space enclosed by the singular surface with the topological charge $N_1 = 1$.

the pole in the Green's function has singularity: the parameter γ in Eq.(5) is nonzero:²⁵

$$G = \frac{Z}{i\omega - \epsilon(\mathbf{p})}, \quad Z \propto (\omega^2 + \epsilon^2(\mathbf{p}))^\gamma. \quad (4)$$

Nevertheless the topological invariant remains the same for all γ : i.e. the Green's function has the same topological property as the Green's function of conventional metal with Fermi surface at $\epsilon(\mathbf{p}) = 0$. This is the reason why the Luttinger theorem is still valid.^{26,27} The particle density of interacting fermions is equal to the volume in the momentum space enclosed by the singular surface

Lifshitz transition from Fermi surface to flat band

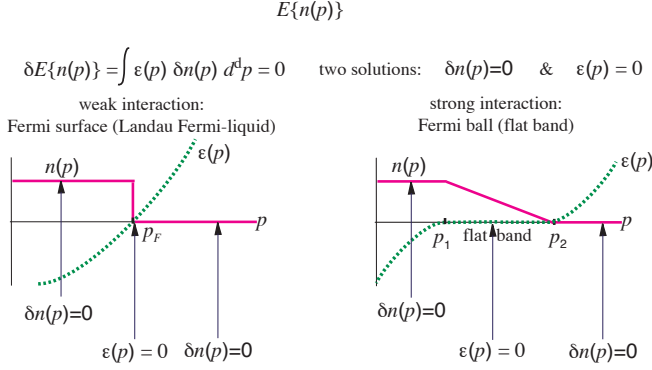


FIG. 6: Formation of flat band in the system of strongly interacting fermions in the Landau theory approach. There are two types of the extrema of the energy functional $E\{n(\mathbf{p})\}$: (i) $\delta n(\mathbf{p}) = 0$, which corresponds to the occupied $n(\mathbf{p}) = 1$ and free $n(\mathbf{p}) = 0$ levels. (ii) $\epsilon(\mathbf{p}) = 0$; this solution takes place when $0 < n(\mathbf{p}) < 1$. On the weak interaction side, the solution (i) takes place inside and the outside the Fermi surface, while the solution (ii) corresponds to the Fermi surface. On the strong interaction side the solution $\epsilon(\mathbf{p}) = 0$ is extended to the 3D band – the flat band. Formation of the flat band from the Fermi surface occurs via the new type of Lifshitz transition.

with the topological charge $N_1 = 1$, irrespective of the realization of the singularity.

The suppression of residue Z can be so strong, that the pole in the Green's function is transformed to the zero of the Green's function, which corresponds to the special case of $\gamma = 1$, see Fig. 5:

$$G \propto i\omega + \epsilon(\mathbf{p}). \quad (5)$$

This situation in particular takes place for Mott insulators,²⁶ which means that the topology of Fermi surface is preserved even in the insulating phase, and thus the Luttinger theorem is still valid.^{26,27} Thus we can say that the transition between metals and insulators can be also viewed as a type of the zero-temperature Lifshitz transition, at which the property of the energy spectrum drastically changes without symmetry breaking. However, this quantum phase transition is not topological since the topological invariant does not change across the transition.

It is not excluded that in the so-called pseudo-gap phase of cuprate superconductors and some other materials, see e.g.²⁸, the part of the Fermi surface transforms to the surface of zeroes and the Fermi arcs are formed, see Fig. 5 (*bottom right*).

D. From Fermi surface to flat band

The flat band – or the so-called Khodel-Shaginyan fermion condensate, where all the states have zero en-

Flat band - route to room-T superconductivity

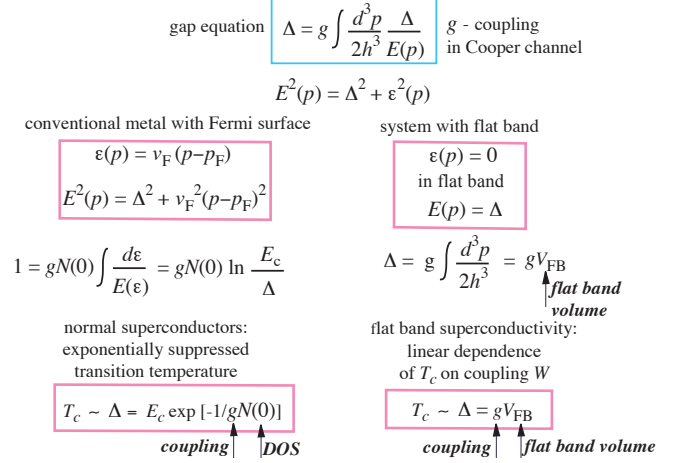


FIG. 7: Flat band of electronic states with zero energy leads to the linear dependence of transition temperature T_c on the coupling parameter,²⁹ while in conventional metals T_c is exponentially suppressed.

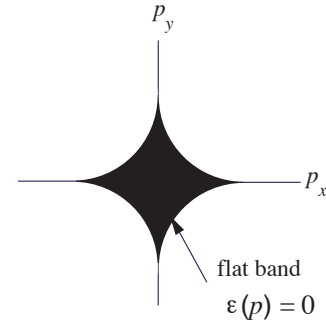


FIG. 8: Flat band emerging in the vicinity of Lifshitz transition in Fig. 4 due to electron-electron interaction.^{34,35} The original non-interacting spectrum is $\epsilon^{(0)}(\mathbf{p}) = p_x p_y / m - \mu$, where the Lifshitz transition takes place at $\mu = 0$. Due to interaction all the states in the black region have zero energy (the flat band is shown at the point of Lifshitz transition).

ergy – is caused by electron-electron interaction.^{29–31} This is the manifestation of the general phenomenon of merging of the energy level due to interaction. Such effect has been observed for Landau levels in 2D quantum wells.^{32,33} Since the flat band has huge density of electronic states, this may considerably enhance the transition temperature to superconducting state, see Fig. 7.

The flat band is more easily formed in the vicinity of the conventional Lifshitz transition,^{34,35} see Fig. 8. Flattening of the single-particle spectrum near the Fermi momentum has been reported in 2D quantum well.³⁶ It is possible that this effect is responsible for the occurrence of superconductivity with high T observed in the pressurized sulfur hydride:^{37,38} there are some theoretical evidences that the high- T_c superconductivity takes place at such pressure, when the system is close to the Lifshitz

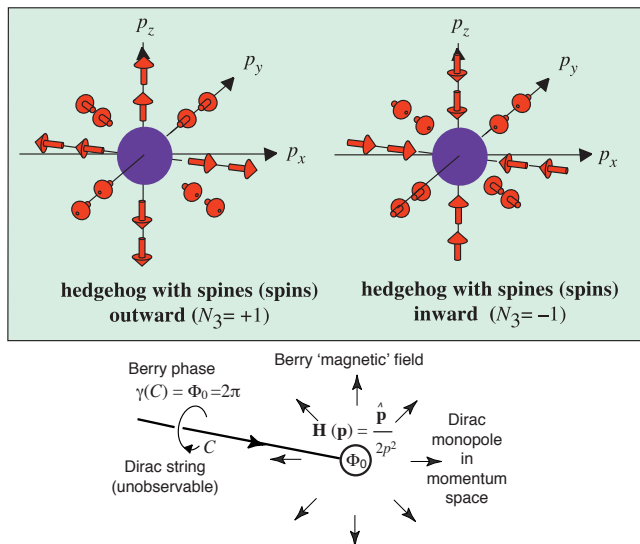


FIG. 9: Spins of the right-handed Weyl particles (quarks and leptons) are directed along the momentum \mathbf{p} forming the hedgehog (*top left*). The anti-hedgehog – the hedgehog with spines (spins) inward (*top right*) corresponds to the left-handed Weyl particles. The topological invariant N_3 describing the topologically distinct hedgehog configurations is expressed either in terms of the Green's function in Eq.(6) or in terms of the unit vector field in Fig. 1 (*center*).

transition.^{39–41} Enhanced superconductivity at Lifshitz transition has been reported in FeSe monolayer.⁴²

III. LIFSHITZ TRANSITIONS GOVERNED BY WEYL POINT TOPOLOGY

A. Topology of Weyl fermions

Weyl particles are the elementary particles of our Universe. The Weyl spinor contains 2 complex components, and these massless particles are described by the 2×2 complex Hamiltonian: $H = c\boldsymbol{\sigma} \cdot \mathbf{p}$ for right-handed quarks and leptons and $H = -c\boldsymbol{\sigma} \cdot \mathbf{p}$ for the left-handed particles, where c is the speed of light. Their spins in momentum space form correspondingly the hedgehog and anti-hedgehog in Fig. 9 (*top*). The hedgehog is the topologically stable object, and thus the Weyl point in the center of the hedgehog is topologically protected. The corresponding topological invariant for the hedgehogs, N_3 , can be expressed in terms of the Green's function as a surface integral in the 3+1 momentum-frequency space $p_\mu = (\mathbf{p}, \omega)$:³

$$N_3 = \frac{\epsilon_{\mu\nu\rho\sigma}}{24\pi^2} \text{tr} \oint_{\Sigma_a} dS^\sigma G \frac{\partial}{\partial p_\mu} G^{-1} G \frac{\partial}{\partial p_\nu} G^{-1} G \frac{\partial}{\partial p_\rho} G^{-1}. \quad (6)$$

Here Σ_a is a three-dimensional surface around the isolated Weyl point in (\mathbf{p}, ω) space.

From the point of view of the general properties of

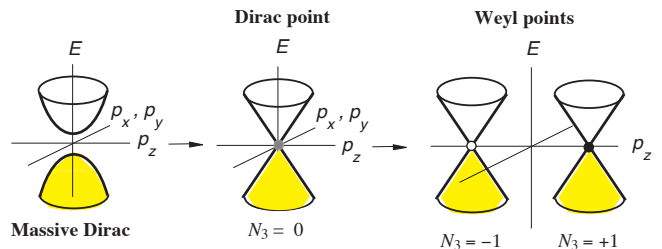


FIG. 10: Formation of the pair of Weyl points from the vacuum state with massive Dirac fermions. Topological charges $N_3 = +1$ and $N_3 = -1$ correspond to right-handed and left-handed particles respectively. At the Lifshitz transition the vacuum is gapless with the Dirac point in the fermionic spectrum which has topological charge $N_3 = 0$.

the fermionic spectrum, the Weyl point represents the exceptional point of level crossing analyzed by von Neumann and Wigner⁴³. This analysis demonstrates that two branches of spectrum, which have the same symmetry, may touch each other at the conical (or diabolical) point in the three-dimensional space of parameters, which in our case are p_x , p_y and p_z . The touching of two branches is described in general by 2×2 Hamiltonian $H = \boldsymbol{\sigma} \cdot \mathbf{g}(\mathbf{p})$. The topological invariant N_3 is expressed in terms of the unit vector $\hat{\mathbf{g}}(\mathbf{p}) = \mathbf{g}(\mathbf{p})/|\mathbf{g}(\mathbf{p})|$ in Fig. 1 (*center*), which forms the hedgehog configuration in Fig. 1 (*middle right*). The touching point also represents the Berry phase monopole in Fig. 9 (*bottom*).⁷ It is not excluded that the Weyl fermions of Standard Model (quark and leptons) are not the elementary particles, but emerge from the level crossing at the more fundamental level.^{2,3,44} In particular, the underlying quantum vacuum can be described by quantum field theory based on real numbers (Majorana fermions), while the imaginary unit, which enters Schrödinger equation, emerges in the low energy limit together with the relativistic linear spectrum of Weyl fermions.⁴⁵

The linear ("relativistic") spectrum emerges only for the elementary topological charges, $N_3 = +1$ or $N_3 = -1$. If the Weyl point has higher topological charge, $|N_3| > 1$, and if there is no special symmetry, which leads to the degeneracy of the levels, the spectrum has different dispersion relations along different axes.^{3,46} For example, for $|N_3| = 2$ the spectrum is "relativistic" in one direction and quadratic in the other two directions.

B. Lifshitz transition with splitting of Weyl points

The typical Lifshitz transition, which involves the Weyl nodes in the fermionic spectrum, describes the formation of the Weyl points with opposite charges $N_3 = \pm 1$ from the fully gapped state. Fig. 10 shows the formation of the pair of the Weyl points from the vacuum state with massive Dirac fermions. The intermediate state has the massless Dirac point in the fermionic spectrum with

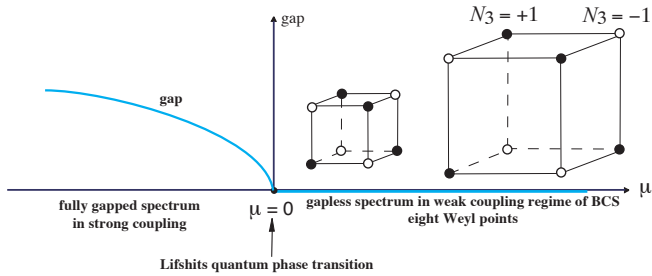


FIG. 11: The BEC to BCS Lifshitz transition with formation of 4 right-handed and 4 left-handed Weyl points at vertices of cube. Such arrangement of the Weyl nodes has been discussed for the energy spectrum in superconductors, which belong to the $O(D_2)$ symmetry class.^{48,49} In relativistic theories a similar arrangement gives 8 left and 8 right Weyl fermions on the vertices of the cube in the 3+1 (p_x, p_y, p_z, ω) space.^{50,51}

topological charge $N_3 = 0$. Such gapless Dirac point is marginal, but can be protected by symmetry as this takes place in Standard Model above the electroweak transition. If the symmetry is violated or is spontaneously broken the Dirac spectrum either acquires mass or splits into the pair of Weyl points.⁴⁷

Fig. 11 demonstrates the formation of 4 right-handed and 4 left-handed Weyl points at the Lifshitz transition between the BEC strong coupling regime to the BCS weak coupling regime. Such arrangement of the Weyl nodes takes place in the energy spectrum in the $O(D_2)$ symmetry class of the pair correlated systems.^{48,49} In both cases the total topological charge $N_3(\text{total}) = 0$, and thus there is an even number of Weyl fermions, which supports the fermion doubling principle.⁵² In relativistic theories the analogical arrangement of 8 left and 8 right Weyl fermions on the vertices of the cube in the 3+1 (p_x, p_y, p_z, ω) space has been discussed.^{50,51} It is interesting that each family of Standard Model fermions contains 8 left and 8 right Weyl particles.

C. Lifshitz transition to type-II Weyl cone

There is the type of Lifshitz transition, which involves both the Fermi surface (invariant N_1) and the Weyl point (invariant N_3). This is the transition between the isolated Fermi points (type-I Weyl spectrum) to the Weyl point connecting two Fermi surfaces (this is called the type-II Weyl point⁵³). In relativistic theories such transitions have been discussed in^{45,54}.

The simplest realization of the type-II Weyl point comes from the following Hamiltonian with two parameters c and v :

$$H = c\boldsymbol{\sigma} \cdot \mathbf{p} - vp_z. \quad (7)$$

For $v = 0$ this is the Weyl point with the Weyl cone in Fig. 12 (top left). For $0 < v < c$ the cone is tilted. At $v > c$ the cone is overtilted, so that the cones cross the

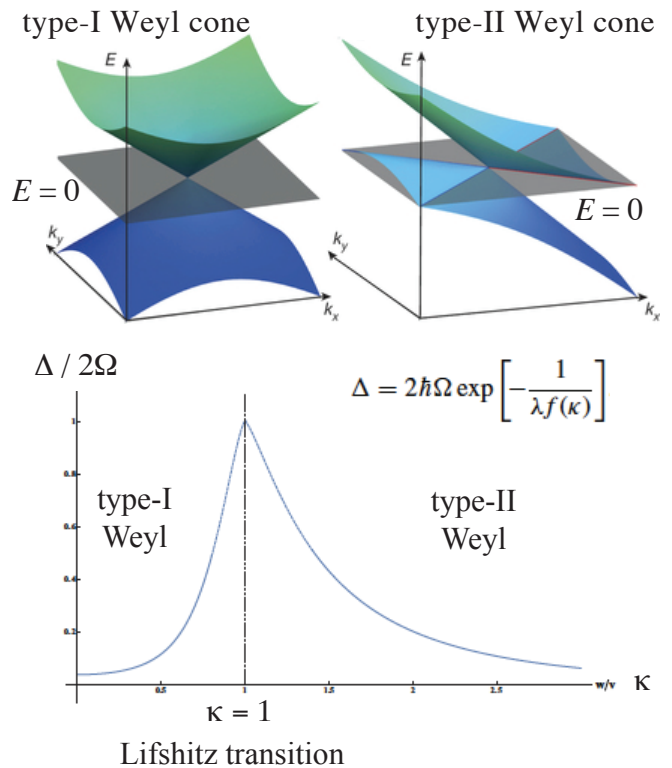


FIG. 12: (top left): Weyl cone in the spectrum of type-I Weyl fermions. (top right): overtilted Weyl cone in the spectrum of type-II Weyl fermions. (bottom): Enhancement of superconducting transition temperature T_c at the Lifshitz transition between the type-I Weyl and the type-II Weyl points.⁵⁵

zero energy level forming two Fermi pockets connected by the Weyl point – the type-II Weyl point, see Fig. 12 (top right). The Lifshitz transition between two types of Weyl point occurs at $v = c$. It is demonstrated that such Lifshitz transition also leads to the enhancement of the transition temperature to superconducting state,^{55,56} see Fig. 12 (bottom).

D. Lifshitz transition at the black hole horizon

Lifshitz transition discussed in Sec. 12 takes place at the black hole horizon. In general relativity the stationary metric, which is valid both outside and inside the black hole horizon, is provided in particular by the Painlevé-Gullstrand spacetime.⁵⁷ The line element of the Painlevé-Gullstrand metric is equivalent to the so-called acoustic metric:^{58–60}

$$ds^2 = g_{\mu\nu} dx^\mu dx^\nu = -c^2 dt^2 + (d\mathbf{r} - \mathbf{v} dt)^2. \quad (8)$$

This metric is expressed in terms of the velocity field $\mathbf{v}(\mathbf{r})$ describing the frame dragging in the gravitational field:

$$\mathbf{v}(\mathbf{r}) = -\hat{\mathbf{r}}c\sqrt{\frac{r_h}{r}}, \quad r_h = \frac{2MG}{c^2}. \quad (9)$$

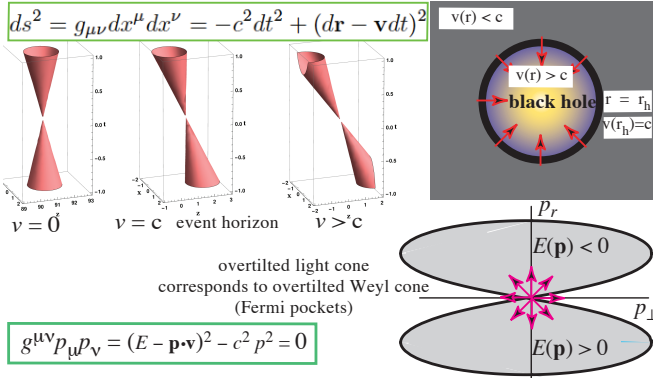


FIG. 13: Black hole in the Painlevé-Gullstrand metric. The metric $g_{\mu\nu}$ describes the light cone. The light cone (*top left*) is overtilted behind the horizon, where the frame drag velocity $v > c$, (*top right*). The metric $g^{\mu\nu}$ describes the Weyl cone. The Weyl cone is overtilted behind the horizon forming two Fermi pockets connected by type-II Weyl point (*bottom*). The horizon at $r = r_h$ serves as the surface of the Lifshitz transition between the type-I Weyl point at $r > r_h$ and the type-II Weyl point at $r < r_h$. This behavior of two cones allow us to simulate the black hole horizon and Hawking radiation using Weyl semimetals.⁶¹

Here M is the mass of the black hole; r_h is the radius of the horizon; G is the Newton gravitational constant. Behind the horizon the drag velocity exceeds the speed of light, $|\mathbf{v}| > c$, and particles are trapped in the hole, see Fig. 13 (*top right*). The behavior of the light cone (the cone in spacetime) across the event horizon is shown in Fig. 13 (*top left*). The light cone is overtilted behind the horizon.

The behavior of the Weyl cone (the cone in momentum space) across the horizon is described by Hamiltonian of the Weyl particles in the gravitational field of the black hole, which for the Painlevé-Gullstrand metric has the following form:⁵⁴

$$H = \pm c\boldsymbol{\sigma} \cdot \mathbf{p} - p_r v(r), \quad v(r) = c\sqrt{\frac{r_h}{r}}. \quad (10)$$

Here the plus and minus signs correspond to the right handed and left handed Weyl fermions respectively; p_r is the radial component of the linear momentum of the particle. Behind the horizon, where $v > c$ and the light cone is overtilted, the Weyl cone is also overtilted, but in the way shown in Fig. 12. Two Fermi pockets are formed, which touch each other at type-II Weyl point in Fig. 13 (*bottom right*). The event horizon at $r = r_h$ thus serves as the surface of the Lifshitz transition.

The correspondence between Weyl semimetals and black holes allows us to simulate the black hole horizon using the inhomogeneous Weyl semimetal, where the transition between the type-I and type-II Weyl points takes place at some surface.⁶¹ This surface would play the role of the event horizon. The formed black hole will be fully stationary in equilibrium. However, just after creation of this black hole analog, the system is not in

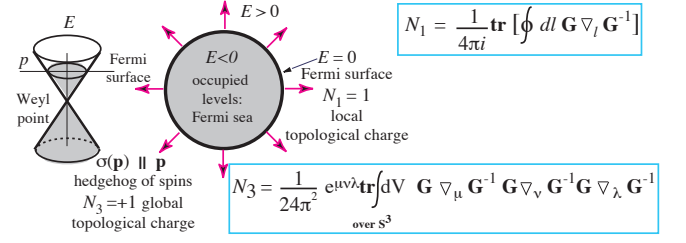


FIG. 14: Fermi surface with local topological charge N_1 and the global topological charge N_3 .³ It contains the Berry phase monopole.

the equilibrium state, and the relaxation process at the initial stage of equilibration looks similar to the process of the Hawking radiation.

In the discussed Lifshitz transition between type-I and type-II Weyl points, the element g_{00} of the effective metric changes sign. Another type of Lifshitz transition occurs when the element g^{00} changes sign. In Weyl semimetals this corresponds to the transition to the type-III Weyl fermions,⁶² while in general relativity this is the transition to spacetimes with closed timelike curves.

IV. LIFSHITZ TRANSITIONS WITH SEVERAL TOPOLOGICAL CHARGES

In sections III C and III D we considered the Lifshitz transition which involved two topological charges: the charge N_1 , which characterizes the Fermi surface, and the charge N_3 of the Berry phase monopole. There are the other Lifshitz transitions with the interplay of these two topological invariants. This happens in particular, when the closed Fermi surface is described by two invariants: the local charge N_1 , which provides the local stability of the Fermi surface, and the global charge N_3 , which describes the Weyl point inside the Fermi surface in Fig. 14. The latter takes place for example when the Weyl point shifts from the zero energy position forming the small Fermi sphere around the Weyl point, see Fig. 14 (*left*). Such Fermi sphere contains the N_3 charge, which can be obtained from Eq.(6) by integration over the surface, which encloses the Fermi sphere.

At the Lifshitz transition the Fermi surfaces can exchange their global charges N_3 or lose the global charge.^{6,47} Example of exchange is in Fig. 15 and the example of the lost global charge is in Fig. 16. In both cases the intermediate state at the point of Lifshitz transition contains the type-II Weyl points.

V. LIFSHITZ TRANSITION GOVERNED BY CONSERVATION OF N_2 CHARGE

The conical Dirac point in the 2D graphene and the nodal lines in the 3D semimetals and nodal superfluids and superconductors are stabilized by the topologi-

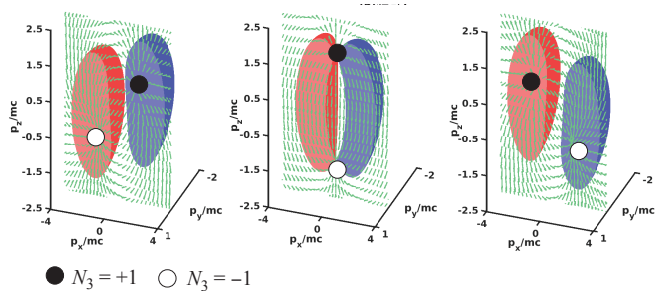


FIG. 15: Lifshitz transition with exchange of Berry phase monopoles between two Fermi surfaces.⁶ The red and the blue Fermi surfaces are globally non-trivial, with $N_3 = -1$ and $N_3 = 1$ respectively. In the process of the Lifshitz transition, two Berry phase monopoles are pushed out from the Fermi surfaces. At the Lifshitz transition the Fermi surfaces touch each other at the Weyl points, so that the latter become the type-II Weyl points. Above the transition the Weyl points are again inside the Fermi surfaces, but now red and the blue Fermi surfaces have the global charges $N_3 = +1$ and $N_3 = -1$ respectively. The topological charges of Fermi surfaces are transferred between the Fermi surfaces via the type-II Weyl points.

cal charge N_2 in Fig. 1 (bottom).^{4,63} Dirac nodal lines were known to exist in the polar phase of superfluid ^3He ,^{8,64} in cuprate superconductors, and in graphite (band crossing lines).⁶⁵⁻⁶⁷ Now they are extensively studied in semimetals.⁶⁸

The type of Lifshitz transitions governed by the conservation of the topological charge N_2 is shown in Fig. 17 on example of bilayer graphene, when one graphene layer is shifted with respect to the other one. Merging of the two conical points with $N_2 = 1$ leads to formation of the Dirac node with quadratic dispersion in Fig. 17 (top left), which has the topological charge $N_2 = 2$. This point in turn may split into four Dirac conical points with $N_2 = \pm 1$ in Fig. 17 (bottom). This is the so-called trigonal warping. The total topological charge is conserved, $N_2 = 1 + 1 + 1 - 1 = 2$. The trigonal warping can be seen in the Bernal graphite, see Fig. 17 (top right), and the transition occurs as a function of p_z ,⁶⁵⁻⁶⁷ when p_z crosses the so-called nexus point.^{63,69}

VI. LIFSHITZ TRANSITIONS BETWEEN GAPPED STATES VIA GAPLESS STATE

Lifshitz transitions between gapped states include transitions between the topological and non-topological insulators; transitions between the fully gapped superfluids/superconductors; transitions between the 2D systems, which experience the intrinsic quantum Hall effect; etc. Here we consider such transition on example of the 2D systems, where the Hall conductance is expressed in terms of the integer-valued topological invariant \tilde{N}_3 in Fig. 18 (top right).⁷⁰⁻⁷³ This topological invariant has the same structure as the invariant N_3 in Fig. 1 (Middle),

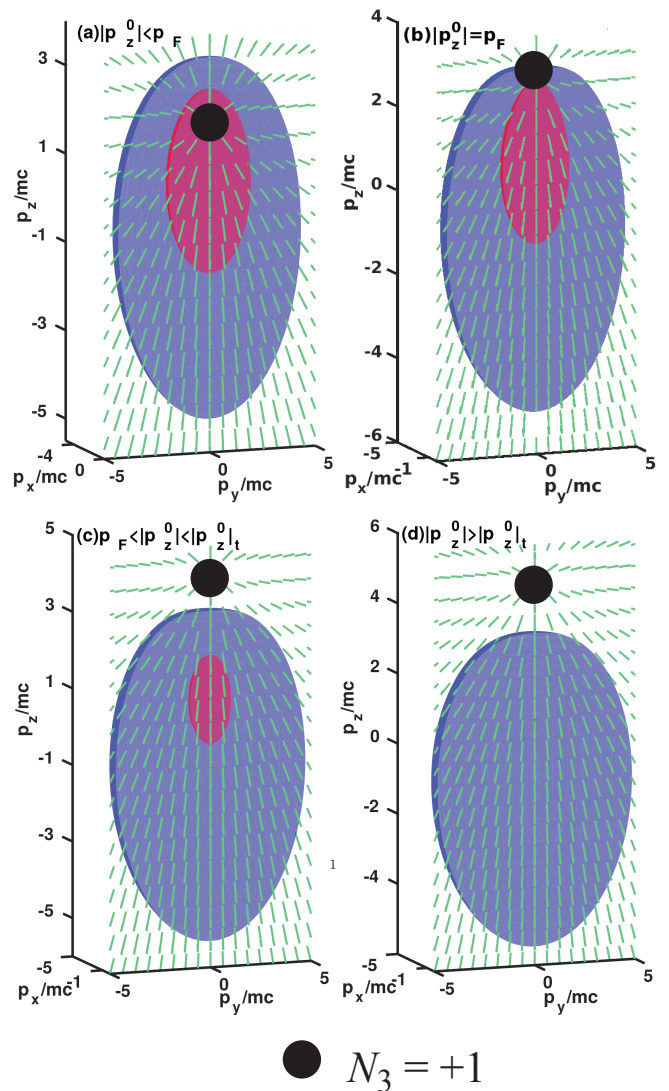


FIG. 16: Lifshitz transition, at which the Fermi surfaces lose the Weyl charge N_3 .⁶ Below the Lifshitz transition both surfaces contain the same Berry phase monopole with $N_3 = +1$. At the transition the Weyl point connects the inner and outer Fermi surfaces. Above the transition the monopole comes out from the Fermi surfaces, and both Fermi surfaces become globally trivial, with $N_3 = 0$. Without global stability the Fermi surface may shrink and disappear in conventional Lifshitz transition as it happens with the red Fermi surface in Fig. 16 (bottom right).

but the integration now is over the whole 2D Brillouin zone. This is an example of the dimensional reduction from the 3D systems with Weyl nodes to the 2D topological insulators.³

Fig. 18 (top left) demonstrates the Lifshitz transition between the topological insulator with $\tilde{N}_3 = 1$ and the trivial insulator with $\tilde{N}_3 = 0$. Here the topological charge is not conserved across the Lifshitz transition, but abruptly changes recalling the first order phase transition. Nevertheless the transition occurs smoothly,

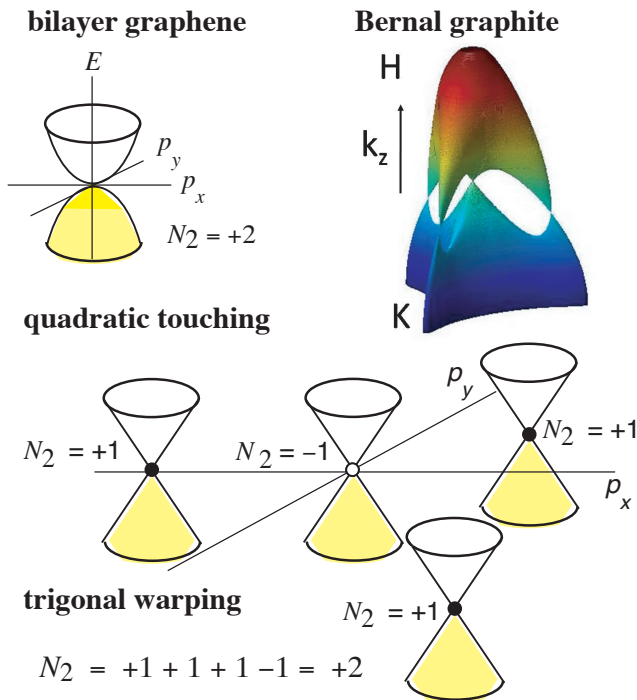


FIG. 17: Lifshitz transition governed by conservation of the topological charge N_2 in bilayer graphene. In bilayer graphene two conical points with the same charge $N_2 = 1$ on two graphene layers are either merge to form the Dirac point with topological charge $N_2 = 2$ with quadratic spectrum in Fig.17 (top left) or split into four Dirac conical points in Fig.17 (bottom). The latter is called the trigonal warping. The total topological charge $N_2 = 2$ in both case and thus one configuration may transform to the other one by Lifshitz transition.

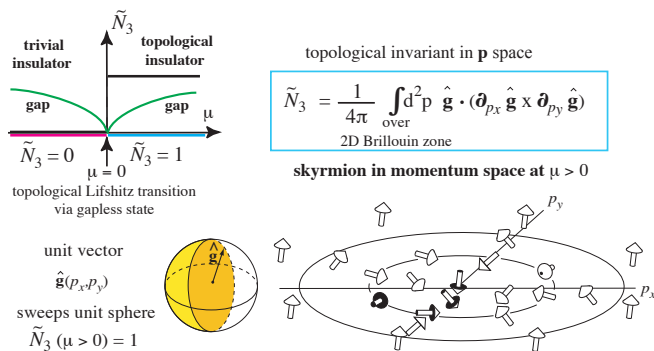


FIG. 18: Lifshitz transition between the fully gapped topologically different vacua in 2D systems, which experiences the intrinsic quantum Hall effect.^{70–74} The Hall conductance is expressed in terms of the integer-valued topological invariant \tilde{N}_3 (top right). The Lifshitz transition between the topological insulator with $\tilde{N}_3 = 1$ and the trivial insulator with $\tilde{N}_3 = 0$ takes place through the state, where the gap vanishes (top left).

(Bottom): The topologically nontrivial state with $\tilde{N}_3 = 1$ represents the topologically nontrivial nonsingular object – skyrmion – in the 2D momentum space.

because at the point of transition the gap in the energy spectrum vanishes. The nullification of the gap at the transition reflects the fact that in the 3D space (p_x, p_y, μ) , where μ is chemical potential or some other parameter along which the transition occurs, the gap node represents the Weyl point with topological charge $N_3 = \tilde{N}_3(\text{right}) - \tilde{N}_3(\text{left})$.^{3,76}

Example is the 2D $p_x + ip_y$ superfluid/superconductor,⁷⁴ where the Lifshitz transition between the superfluid states with $\tilde{N}_3 = 1$ and $\tilde{N}_3 = 0$ occurs at the same point $\mu = 0$ as in the normal Fermi liquid. The detailed consideration shows that the Lifshitz transition represents the quantum transition of third order:⁷⁵ the third-order derivative d^3E/dg^3 of the ground state energy E over the interaction strength g is discontinuous. Compare this with the original $2\frac{1}{2}$ order transition,¹ and the $3\frac{1}{2}$ order transition discussed recently.⁶⁵

The nullification of the gap in the fermionic spectrum at the transition between the gapped vacua, suggests the scenario for the solution of the hierarchy problem: the relativistic quantum vacuum is almost massless because our Universe is very close to the line of the Lifshitz transition. The reason why nature would prefer the critical line may be that the gapless states on the transition line are able to accommodate more entropy than the gapped states.¹⁰

VII. CONCLUSION

Topological Lifshitz transitions are ubiquitous, since they involve many types of the topological structure of fermionic spectrum: Fermi surfaces, Dirac lines, Dirac and Weyl points, edge states, Majorana zero modes, etc. Each of these structures has their own topological invariant, such as $N_1, N_2, N_3, \tilde{N}_3$, etc., which supports the stability of a given class of the topological structure. The topology of the shape of the Fermi surfaces and the Dirac lines, as well as the interconnection of the objects of different dimensionalities in momentum and frequency-momentum spaces, lead to numerous classes of Lifshitz transitions.

The consequences of Lifshitz transitions are important in different areas of physics. In particular, the singular density of electronic states emerging at the transition is important for the construction of superconductors with enhanced transition temperature; the Lifshitz transition can be in the origin of the small masses of elementary particles in our Universe; the black hole horizon serves as the surface of Lifshitz transition between the vacua with type-I and type-II Weyl points; etc.

Acknowledgements

The work has been supported by the European Research Council (ERC) under the European Union's Hori-

zon 2020 research and innovation programme (Grant Agreement No. 694248) and by RSCF (No. 16-42-

01100).

- ¹ I.M. Lifshitz, Anomalies of electron characteristics of a metal in the high pressure region, *Sov. Phys. JETP* **11**, 1130 (1960).
- ² P. Hořava, Stability of Fermi surfaces and K -theory, *Phys. Rev. Lett.* **95**, 016405 (2005).
- ³ G.E. Volovik, *The Universe in a Helium Droplet*, Clarendon Press, Oxford (2003).
- ⁴ G.E. Volovik, Quantum phase transitions from topology in momentum space, *Springer Lecture Notes in Physics* **718**, 31–73 (2007); [cond-mat/0601372](https://arxiv.org/abs/cond-mat/0601372).
- ⁵ G.E. Volovik, Topological Lifshitz transitions, *Fizika Nizkikh Temperatur* **43**, 57–67 (2017), [arXiv:1606.08318](https://arxiv.org/abs/1606.08318).
- ⁶ Kuang Zhang and G.E. Volovik, Lifshitz transitions via the type-II Dirac and type-II Weyl points, *Pis'ma ZhETF* **105**, 504–505 (2017), *JETP Lett.* **105**, 519–525 (2017).
- ⁷ G.E. Volovik, Zeros in the fermion spectrum in superfluid systems as diabolical points, *JETP Lett.* **46**, 98–102 (1987).
- ⁸ V.V. Dmitriev, A.A. Senin, A.A. Soldatov, and A.N. Yudin, Polar phase of superfluid ^3He in anisotropic aerogel, *Phys. Rev. Lett.* **115**, 165304 (2015).
- ⁹ C.D. Froggatt and H.B. Nielsen, *Origin of Symmetry*, World Scientific, Singapore, 1991.
- ¹⁰ G.E. Volovik, Topological invariants for Standard Model: from semi-metal to topological insulator, *Pis'ma ZhETF* **91**, 61–67 (2010); *JETP Lett.* **91**, 55–61 (2010); [arXiv:0912.0502](https://arxiv.org/abs/0912.0502).
- ¹¹ B.G. Sidharth, A. Das, C.R. Das, L.V. Laperashvili and H.B. Nielsen, Topological structure of the vacuum, cosmological constant and dark energy, *Int. J. Mod. Phys. A* **31**, 1630051 (2016), [arXiv:1605.01169](https://arxiv.org/abs/1605.01169).
- ¹² B.G. Sidharth, A. Das, C.R. Das, L.V. Laperashvili and H.B. Nielsen, Cosmological constant and the vacuum stability in the Standard Model, *New Advances in Physics* **10**, 1–39 (2016).
- ¹³ L.V. Laperashvili, H.B. Nielsen and C.R. Das, New results at LHC confirming the vacuum stability and Multiple Point Principle, *Int. J. Mod. Phys. A* **31**, 1650029 (2016).
- ¹⁴ D.L. Bennett, H.B. Nielsen and C.D. Froggatt, Standard model parameters from the multiple point principle and anti-GUT, [arXiv:hep-ph/9710407](https://arxiv.org/abs/hep-ph/9710407).
- ¹⁵ G.E. Volovik, Coexistence of different vacua in the effective quantum field theory and multiple point principle, *JETP Lett.* **79**, 101 (2004), *Pisma ZhETF* **79**, 131 (2004), [arXiv:hep-ph/0309144](https://arxiv.org/abs/hep-ph/0309144).
- ¹⁶ G.E. Volovik, Zeroes in energy gap in superconductors with high transition temperature, *Phys. Lett. A* **142**, 282–284 (1989).
- ¹⁷ W.V. Liu and F. Wilczek, Interior gap superfluidity, *Phys. Rev. Lett.* **90**, 047002 (2003).
- ¹⁸ V. Barzykin and L.P. Gor'kov, Gapless Fermi surfaces in superconducting CeCoIn_5 , *Phys. Rev. B* **76**, 014509 (2007).
- ¹⁹ D.F. Agterberg, P.M.R. Brydon, C. Timm, Bogoliubov Fermi surfaces in superconductors with broken time-reversal symmetry, *Phys. Rev. Lett.* **118**, 127001 (2017).
- ²⁰ C. Timm, A.P. Schnyder, D.F. Agterberg, and P.M.R. Brydon, Inflated nodes and surface states in superconducting half-Heusler compounds, [arXiv:1707.02739](https://arxiv.org/abs/1707.02739).
- ²¹ G.E. Volovik, Superfluid properties of the A-phase of ^3He , *Usp. Fiz. Nauk.* **143**, 73–109; *Soviet Phys. Usp.* **27**, 363–384.
- ²² J.T. Mäkinen, S. Autti, V.B. Eltsov, J. Rysti and G.E. Volovik, Vortex non-dynamics and exceeding the Landau speed limit in the polar phase of superfluid ^3He , 28th International Conference on Low Temperature Physics, LT28, abstract 008, <http://www.trippus.se/eventus/userfiles/84948.pdf>
- ²³ D. Vollhardt, K. Maki and N. Schopohl, Anisotropic gap distortion due to superflow and the depairing critical current in superfluid $^3\text{He-B}$, *J. Low Temp. Phys.* **39**, 79–92 (1980).
- ²⁴ T. Zhu, M.L. Evans, R.A. Brown, P.M. Walmsley, and A.I. Golov, Interactions between unidirectional quantized vortex rings, *Phys. Rev. Fluids* **1**, 044502 (2016).
- ²⁵ J. Voit, One-dimensional Fermi liquids, *Reports on Progress in Physics* **58**, 977 (1995).
- ²⁶ I. Dzyaloshinskii: Some consequences of the Luttinger theorem: The Luttinger surfaces in non-Fermi liquids and Mott insulators, *Phys. Rev. Phys. Rev. B* **68**, 085113 (2003).
- ²⁷ B. Farid, A.M. Tselik, Comment on "Breakdown of the Luttinger sum rule within the Mott-Hubbard insulator", by J. Kokalj and P. Prelovsek [*Phys. Rev. B* **78**, 153103 (2008), [arXiv:0803.4468](https://arxiv.org/abs/0803.4468)], [arXiv:0909.2886](https://arxiv.org/abs/0909.2886).
- ²⁸ U.S. Pracht, N. Bachar, L. Benfatto, G. Deutscher, E. Farber, M. Dressel and M. Scheffler, Enhanced Cooper pairing versus suppressed phase coherence shaping the superconducting dome in coupled aluminum nanograins, *Phys. Rev. B* **93**, 100503(R) (2016).
- ²⁹ V.A. Khodel and V.R. Shaginyan, Superfluidity in system with fermion condensate, *JETP Lett.* **51**, 553 (1990).
- ³⁰ G.E. Volovik, A new class of normal Fermi liquids, *JETP Lett.* **53**, 222 (1991).
- ³¹ P. Nozieres, Properties of Fermi liquids with a finite range interaction, *J. Phys. (Fr.)* **2**, 443–458 (1992).
- ³² A.A. Shashkin, V.T. Dolgoplov, J.W. Clark, V.R. Shaginyan, M.V. Zverev, V.A. Khodel, Merging of Landau levels in a strongly-interacting two-dimensional electron system in silicon, *Phys. Rev. Lett.* **112**, 186402 (2014).
- ³³ A.A. Shashkin, V.T. Dolgoplov, J.W. Clark, V.R. Shaginyan, M.V. Zverev, V.A. Khodel, Interaction-induced merging of Landau levels in an electron system of double quantum wells, *JETP Letters* **102**, 36 (2015)
- ³⁴ D. Yudin, D. Hirschmeier, H. Hafermann, O. Eriksson, A.I. Lichtenstein and M.I. Katsnelson, Fermi condensation near van Hove singularities within the Hubbard model on the triangular lattice, *Phys. Rev. Lett.* **112**, 070403 (2014).
- ³⁵ G.E. Volovik, On Fermi condensate: near the saddle point and within the vortex core, *Pis'ma ZhETF* **59**, 798–802 (1994); *JETP Lett.* **59**, 830–835 (1994).
- ³⁶ M.Yu. Melnikov, A.A. Shashkin, V.T. Dolgoplov, S.-H. Huang, C.W. Liu, S.V. Kravchenko, Indication of the fermion condensation in a strongly correlated electron system in SiGe/Si/SiGe quantum wells, [arXiv:1604.08527](https://arxiv.org/abs/1604.08527).

- ³⁷ A.P. Drozdov, M.I. Erements, I.A. Troyan, V. Ksenofontov, S.I. Shylin, Conventional superconductivity at 203 K at high pressures, *Nature* **525**, 73 (2015).
- ³⁸ M.I. Erements and A.P. Drozdov, High-temperature conventional superconductivity, *Phys. Usp.* **59** 1154–1160 (2016).
- ³⁹ Yundi Quan and Warren E. Pickett, Impact of van Hove singularities in the strongly coupled high temperature superconductor H₃S, *Phys. Rev. B* **93**, 104526 (2016).
- ⁴⁰ A. Bianconi and T. Jarlborg, Lifshitz transitions and zero point lattice fluctuations in sulfur hydride showing near room temperature superconductivity, *Novel Superconducting Materials* **1**, 37–49 (2015); arXiv:1507.01093.
- ⁴¹ T.X.R. Souza, F. Marsiglio, The possible role of van Hove singularities in the high T_c of superconducting H₃S, arXiv:1708.07264.
- ⁴² X. Shi, Z.-Q. Han, X.-L. Peng, P. Richard, T. Qian, X.-X. Wu, M.-W. Qiu, S.C. Wang, J.P. Hu, Y.-J. Sun, H. Ding, Enhanced superconductivity accompanying a Lifshitz transition in electron-doped FeSe monolayer, *Nature Communications* **8**, 14988 (2017).
- ⁴³ J. von Neumann und E.P. Wigner, Über das Verhalten von Eigenwerten bei adiabatischen Prozessen, *Phys. Zeit.* **30**, 467–470 (1929).
- ⁴⁴ C.D. Froggatt and H.B. Nielsen, *Origin of Symmetry* (World Scientific, Singapore, 1991).
- ⁴⁵ G.E. Volovik and M.A. Zubkov, Emergent Weyl spinors in multi-fermion systems, *Nuclear Physics B* **881**, 514–538 (2014).
- ⁴⁶ G.E. Volovik, V.A. Konyshov, Properties of the superfluid systems with multiple zeros in fermion spectrum, *Pisma ZhETF* **47**, 207–209 (1988); *JETP Lett.* **47**, 250–254 (1988).
- ⁴⁷ F.R. Klinkhamer and G.E. Volovik, Emergent CPT violation from the splitting of Fermi points, *Int. J. Mod. Phys. A* **20**, 2795–2812 (2005); hep-th/0403037.
- ⁴⁸ G.E. Volovik, L.P. Gor'kov, Superconductivity classes in the heavy fermion systems, *JETP* **61**, 843–854 (1985).
- ⁴⁹ G.E. Volovik, Dirac and Weyl fermions: from Gor'kov equations to Standard Model (in memory of Lev Petrovich Gorkov), *Pis'ma ZhETF* **105**, 245–246 (2017), *JETP Lett.* **105**, 273–277 (2017), arXiv:1701.01075.
- ⁵⁰ M. Creutz, Four-dimensional graphene and chiral fermions, *JHEP* 0804:017 (2008).
- ⁵¹ M. Creutz, Emergent spin, *Annals Phys.* **342**, 21–30 (2014).
- ⁵² H.B. Nielsen, M. Ninomiya: Absence of neutrinos on a lattice. I - Proof by homotopy theory, *Nucl. Phys. B* **185**, 20 (1981); Absence of neutrinos on a lattice. II - Intuitive homotopy proof, *Nucl. Phys. B* **193**, 173 (1981).
- ⁵³ A.A. Soluyanov, D. Gresch, Zhijun Wang, QuanSheng Wu, M. Troyer, Xi Dai, B.A. Bernevig, Type-II Weyl semimetals, *Nature* **527**, 495–498 (2015).
- ⁵⁴ P. Huhtala and G.E. Volovik, Fermionic microstates within Painlevé-Gullstrand black hole, *ZhETF* **121**, 995-1003; *JETP* **94**, 853-861 (2002); gr-qc/0111055.
- ⁵⁵ Dingping Li, B. Rosenstein, B.Ya. Shapiro, and I. Shapiro, Effect of the type-I to type-II Weyl semimetal topological transition on superconductivity, *Phys. Rev. B* **95**, 094513 (2017).
- ⁵⁶ M. Alidoust, K. Halterman, and A. A. Zyuzin, Superconductivity in type-II Weyl semimetals, *Phys. Rev. B* **95**, 155124 (2017).
- ⁵⁷ P. Painlevé, La mécanique classique et la théorie de la relativité, *C. R. Hebd. Acad. Sci. (Paris)* **173**, 677-680 (1921); A. Gullstrand, Allgemeine Lösung des statischen Einkörperproblems in der Einsteinschen Gravitationstheorie, *Arkiv. Mat. Astron. Fys.* **16**, 1-15 (1922).
- ⁵⁸ W.G. Unruh, Experimental Black-Hole Evaporation, *Phys. Rev. Lett.* **46**, 1351 (1981).
- ⁵⁹ W.G. Unruh, Sonic analogue of black holes and the effects of high frequencies on black hole evaporation, *Phys. Rev. D* **51**, 2827–2838 (1995).
- ⁶⁰ P. Kraus and F. Wilczek, Some applications of a simple stationary line element for the Schwarzschild geometry, *Mod. Phys. Lett. A* **9**, 3713–3719 (1994).
- ⁶¹ G.E. Volovik, Black hole and Hawking radiation by type-II Weyl fermions, *Pisma ZhETF* **104**, 660–661 (2016), *JETP Lett.* **104**, 645–648 (2016), arXiv:1610.00521.
- ⁶² J. Nissinen and G.E. Volovik, Type-III and IV interacting Weyl points, *Pisma ZhETF* **105**, 442–443 (2017), *JETP Lett.* **105**, 447–452 (2017), arXiv:1702.04624.
- ⁶³ T.T. Heikkilä and G.E. Volovik, Nexus and Dirac lines in topological materials, *New J. Phys.* **17**, 093019 (2015), arXiv:1505.03277.
- ⁶⁴ S. Autti, V.V. Dmitriev, J.T. Mäkinen, A.A. Soldatov, G.E. Volovik, A.N. Yudin, V.V. Zavjalov, and V.B. Eltsov, Observation of half-quantum vortices in superfluid ³He, *Phys. Rev. Lett.* **117**, 255301 (2016).
- ⁶⁵ G.P. Mikitik and Yu.V. Sharlai, Dirac points of electron energy spectrum, band-contact lines, and electron topological transitions of 3½ kind in three-dimensional metals, *Phys. Rev. B* **90**, 155122 (2014).
- ⁶⁶ G.P. Mikitik and Yu.V. Sharlai, Band-contact lines in the electron energy spectrum of graphite, *Phys. Rev. B* **73**, 235112 (2006).
- ⁶⁷ G.P. Mikitik and Yu.V. Sharlai, The Berry phase in graphene and graphite multilayers, *Low Temp. Phys.* **34**, 794–780 (2008).
- ⁶⁸ D. Takane, K. Nakayama, S. Souma, T. Wada, Y. Okamoto, K. Takenaka, Y. Yamakawa, A. Yamakage, T. Mitsuhashi, K. Horiba, H. Kumigashira, T. Takahashi, and T. Sato, Observation of Dirac-like energy band and ring-torus Fermi surface in topological line-node semimetal CaAgAs, arXiv:1708.06874.
- ⁶⁹ T. Hyart, T. T. Heikkilä, Momentum-space structure of surface states in a topological semimetal with a nexus point of Dirac lines, *Phys. Rev. B* **93**, 235147 (2016).
- ⁷⁰ H. So, Induced topological invariants by lattice fermions in odd dimensions, *Prog. Theor. Phys.* **74**, 585–593 (1985).
- ⁷¹ K. Ishikawa and T. Matsuyama, Magnetic field induced multi component QED in three-dimensions and quantum Hall effect, *Z. Phys. C* **33**, 41–45 (1986).
- ⁷² K. Ishikawa and T. Matsuyama, A microscopic theory of the quantum Hall effect, *Nucl. Phys. B* **280**, 523–548 (1987).
- ⁷³ F.D.M. Haldane, Model for a quantum Hall effect without Landau levels: Condensed-matter realization of the "Parity Anomaly", *Phys. Rev. Lett.* **61**, 2015–2018 (1988).
- ⁷⁴ G.E. Volovik, Analog of quantum Hall effect in superfluid ³He film, *JETP* **67**, 1804–1811 (1988).
- ⁷⁵ S.M.A. Rombouts, J. Dukelsky and G. Ortiz, Quantum phase diagram of the integrable $p_x + ip_y$ fermionic superfluid, *Phys. Rev. B* **82**, 224510 (2010).
- ⁷⁶ S. Kourtis, T. Neupert, C. Mudry, M. Sigrist, and Wei Chen, Weyl-type topological phase transitions in fractional quantum Hall-like systems, arXiv:1708.04244.